Cellular Microbiology (2005) 7(1), 115–127 doi:10.1111/j.1462-5822.2004.00441.x

Intravenous infection of virulent shigellae causes fulminant hepatitis in mice

Maria Celeste Martino,[1] Giacomo Rossi,[2] Ivan Tattoli,[1] Irene Martini,[1] Damiana Chiavolini,[3] Giancarlo Cortese,[4] Gianni Pozzi[3] and Maria Lina Bernardini[1]*

[1]*Dipartimento di Biologia Cellulare e dello Sviluppo, Sezione di Scienze Microbiologiche, Università 'La Sapienza', Via dei Sardi 70, 00185 Roma, Italy.*
[2]*Facoltà di Medicina Veterinaria, Università di Camerino, Matelica, Italy.*
[3]*Dipartimento di Microbiologia, Università di Siena, Italy.*
[4]*Istituto Regina Elena, Roma, Italy.*

Summary

Shigella **spp. are pathogenic bacteria responsible for bacillary dysentery in humans. The major lesions in colonic mucosa are intense inflammation with apoptosis of macrophages and release of pro-inflammatory cytokines. The study of shigellosis is hindered by the natural resistance of rodents to oral infection with *Shigella*. Therefore, animal models exploit other routes of infection. Here, we describe a novel murine model in which animals receive shigellae via the caudal vein. Mice infected with 5×10^6 (LD_{50}) virulent shigellae died at 48 h post infection, whereas animals receiving non-invasive mutants survived. The liver is the main target of infection, where shigellae induce microgranuloma formation. In mice infected with invasive bacteria, high frequency of apoptotic cells is observed within hepatic microgranulomas along with significant levels of mRNA for pro-inflammatory cytokines such as IL-1β, IL-18, IL-12 and IFN-γ. Moreover, in the blood of these animals high levels of IL-6 and transaminases are detected. Our results demonstrate the intravenous model is suitable for pathogenicity studies and useful to explore the immune response after *Shigella* infection.**

Introduction

Shigella flexneri is the major aetiological agent of endemic bacillary dysentery, a severe form of diarrhoea responsible for ≈1 million fatalities annually (Kotloff *et al*., 1999). After oral ingestion of as few as 100 shigellae, these microorganisms reach the colonic lumen and proceed to invade the mucosa by translocating through M-cells of the follicle-associated epithelium (FAE) that covers solitary lymphoid nodules dispersed throughout the colorectal surface (Sansonetti *et al*., 1991). From this initial site of invasion, bacteria penetrate intestinal epithelial cells (IECs) into which they inject effector proteins (Ipa) via a type III secretion apparatus (Buttner and Bonas, 2002); the bacteria's genes are located on a large virulence plasmid common to all *Shigella* spp. (Sansonetti *et al*., 1982). Upon Nod-1-mediated peptidoglycan recognition, infected IECs activate NF-κB inducing the release of pro-inflammatory cytokines and chemokines (Girardin *et al*., 2003), especially IL-8 (Philpott *et al*., 2000). Then, infected macrophages undergo apoptosis through the activation of caspase-1 (Zychlinsky *et al*., 1992; Hilbi *et al*., 1998) that stimulates the release of further pro-inflammatory factors such as IL-1β and IL-18 (Zychlinsky *et al*., 1994; Chen *et al*., 1996; Sansonetti *et al*., 2000). Finally, polymorphonuclear (PMN) leukocytes are recruited to the sites of invasion (Perdomo *et al*., 1994; Sansonetti *et al*., 1999), and eventually eliminate invasive bacteria, blocking their escape from the phagocytic vacuole in which they are killed (Mandic-Mulec *et al*., 1997; Weinrauch *et al*., 2002). Thus, shigellosis is a disease that results from a dysregulated inflammatory response of the host to the presence of a limited amount of pathogen. The intense inflammatory reaction prevents the septicaemic dissemination of shigellae at the price of lesions and abscesses in the colonic tissue. From this point of view, improving the knowledge about the host mechanisms triggered by invading shigellae may provide fundamental information on the cascade of events underlying the activation of inflammation in response to bacteria exposure. However, there is no animal model that fully mimics the pathogenesis of shigellosis. Therefore, alternative systems have been applied to model natural shigellosis. In the murine pulmonary model of shigellosis, mice develop a severe pneumonia (Voino-Yasenetsky and Voino-Yasenetskaya, 1962) after intranasal administration of bacteria. The study of the pulmonary shigellosis has provided valuable information about the basic mechanisms of *Shigella* immunity (Phalipon *et al*., 1995); however, the strong inflammatory reaction of the pulmonary tissue

Received 27 February, 2004; revised 1 June, 2004; accepted 25 June, 2004. *For correspondence. E-mail MariaLina.Bernardini@uniroma1.it; Tel. (+39) 06 49917579/49917850; Fax (+39) 06 49917594.

makes it difficult to use this model in the comparative analyses of the *Shigella* mutants. In the rabbit ligated ileal loop model (Formal *et al.*, 1961) the constraints include the need for surgery and the paucity of immunological reagents for rabbit cells. The Sereny test, in which infection elicits keratoconjunctivitis in guinea pigs, has the same limitations (Sereny, 1957). The recently developed newborn mouse model of intestinal infection (Fernandez *et al.*, 2003) induces acute intestinal inflammation and massive tissue destruction, partially mimicking the natural disease. This model is extremely sensitive to the age of mice: in order to develop the disease, the animals have to be infected in the fourth day from birth. Therefore, although the analysis of newborn mouse intestinal tissues will certainly prove to be useful to analyse some aspects of *Shigella* pathogenesis, its use in routine studies appears to be doubtful.

The only model that mimics natural shigellosis in humans is the intragastric infection of *Macacus rhesus* (Takeuchi *et al.*, 1975). However, the scarcity of non-human primates, their cost and major ethical concerns make these animals unsuitable for studying shigellosis on a routine basis. In conclusion, the relevance of the study of a mouse model of shigellosis is likely to continue to remain a crucial target of the search for *in vivo* models.

We have previously observed that in guinea pigs infected intragastrically with shigellae, wild-type bacteria and mutants were isolated from liver (Bernardini *et al.*, 2001). Likewise, in rabbit infected via this same route, shigellae disseminate into the liver (Etheridge *et al.*, 1996). Hepatitis after *Shigella* infection has also been recorded in humans (Stern and Gitnik, 1976). Starting from these premises, in this study we have addressed the question of whether the liver could be a primary target of *Shigella* infection and whether its colonization could mimic some events occurring in natural shigellosis. To this aim, we have established a new experimental mouse model of *Shigella* infection in which the animals received *Shigella* intravenously (i.v.) directly through the caudal vein. We have therefore proceeded to the analysis of: (i) mice mortality, (ii) bacterial survival in blood and dissemination throughout organs and (iii) lesions induced in the liver and inflammatory reaction. The results demonstrate that our systemic model of infection in mice reproduces some as yet unknown steps of *Shigella* pathogenesis thus providing a useful tool to elucidate the mechanisms underlying the inflammatory response.

Results

Intravenous injection of invasive shigellae causes death of mice

The wild-type strain M90T or its non-invasive, plasmidless variant, BS176, was inoculated i.v. into the caudal vein of 5-week-old BALB/C mice. In preliminary experiments, different doses of cfu per mouse, such as 10^5, 10^6, 5×10^6, 8×10^6, 10^7, 5×10^7, 10^8 and 10^9, were given of each strain, and a dose/mortality curve was constructed (Fig. 1). Mice were observed for 96 h post infection (p.i.), and death was recorded up to 48 h. At the dose of 10^7 cfu, a 80% mortality was observed with M90T; all mice inoculated with higher doses died. In contrast, after challenge with BS176 mice died at doses higher than 10^8 cfu, 25% mortality being observed with 10^9 cfu (Fig. 1A). Therefore, LD_{50} is 5×10^6 cfu per mouse for M90T, whereas there was no LD_{50} for BS176 at the experimental doses.

Shigellae colonize liver and spleen

In preliminary analyses after challenge with 10^7 cfu of M90T, bacteria were mainly isolated from the liver and spleen of animals at 12, 24 and 48 h p.i., whereas only

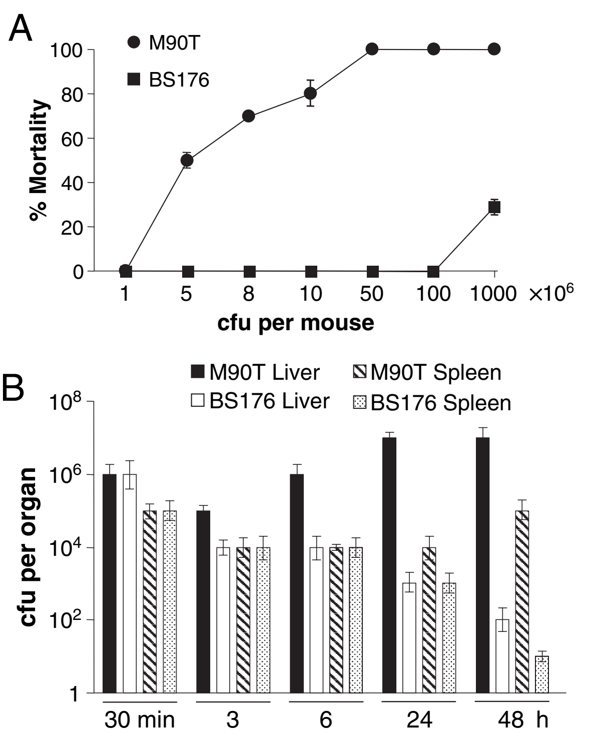

Fig. 1. Mice mortality and organ colonization after intravenous (i.v.) infection of shigellae.
A. Dose/mortality curve. Mice were inoculated i.v. with increasing doses of M90T and BS176. LD_{50} for M90T was set at 5×10^6 cfu per mouse. No LD_{50} could be established for BS176. Lethality was assessed over a period of 96 h (no deaths occurred after 48 h). Data are pooled results ± SD of three experiments in which $n = 6$ for each dose of M90T and BS176 in individual experiments.
B. Recovery of bacteria from liver and spleen. Liver and spleen of mice that survived at 48 h after i.v. infection with M90T and BS176 were examined for the presence of shigellae. Results, given as cfu per organ, represent the mean of three experiments ± SD. cfu in the liver of animals infected with M90T versus cfu in the liver of mice infected with BS176 at 24 and 48 h, $P < 0.0001$ (Student's *t*-test).

few bacteria were recovered from kidneys and lungs (data not shown). Therefore, we analysed the kinetics of bacterial colonization of these organs at early times of infection with 10^7 cfu of M90T or BS176. Six mice infected with either M90T or BS176, were sacrificed at 30 min, 3, 6, 24 and 48 h p.i. The liver and the spleen were removed to evaluate the number of bacteria and to proceed to the histopathological and immunohistochemical analyses. After 30 min of infection with BS176, the number of cfu was 10^6 in the liver and 10^5 in the spleen. At 48 h p.i., the number of cfu decreased to 10^2 in the liver and to 10 in the spleen. The kinetics of colonization of the liver and the spleen in mice infected with M90T followed a different trend. At 30 min p.i., the number of cfu isolated from the liver and the spleen was 10^6 and 10^5, respectively, like with BS176. At 3 h p.i., the amount of bacteria in the liver and the spleen slightly decreased (10^5 and 10^4 cfu) to return to the initial level at 6 h p.i. Finally, at 48 h p.i. in surviving mice, we found about 10^7 cfu in the liver and 10^5 cfu in the spleen. Data are shown in Fig. 1B.

To test for the presence of shigellae in the blood, blood samples taken at different time points were separately plated on solid media (TSA). The amount of bacteria recovered at 1, 3, 6 and 12 h was almost constant (about 300 cfu ml^{-1} for M90T and 50 cfu ml^{-1} for BS176). At 24 h M90T only was recovered (100 cfu ml^{-1}), and at 48 h less than 10 cfu ml^{-1} of both strains were present.

The presence of shigellae in the liver induces microgranuloma formation

In pilot experiments major histopathological lesions were observed in surviving animals at 48 h p.i. with M90T. Therefore, only this time point was considered in further histopathological studies. In M90T-inoculated mice, the liver had a mottled appearance by macroscopic inspection. Histopathological analysis revealed severe degeneration and cloudy swelling of hepatocytes. Necrotic areas in which cellular morphology was completely altered were also present. Interestingly, several microgranulomas were observed with mononuclear cell aggregates and interspersed neutrophils that infiltrated massively into pericentrolobular tracts. These aggregates, consisting of focal leukocyte reaction (i.e. epithelioid and lymphoid cells) and hepatic cell death, had central areas of mild necrosis, with many hepatocytes having picnotic nuclei (Fig. 2A).

Some mononuclear cells, i.e. Kupffer cells and non-resident macrophages, were observed by using monoclonal antibody (mAb) specific for anti-*S. flexneri* LPS, particularly in livers of mice infected with M90T (Figs 2B and 3A). Moreover, triple immunohistochemical stain revealed many CD3+ lymphocytes and macrophages, positive for both anti-*S. flexneri* LPS mAb and anti-F4/80 mAb (Fig. 2B). In contrast, little, if any, infiltration of mononuclear cells was observed in livers of mice infected with BS176 (Fig. 2C). These livers retained a normal structure with, in some cases, small aggregates of macrophages and lymphoid cells containing a few CD3+ lymphocytes (Fig. 2D). However, necrotic foci or hepatocyte swelling was not observed. Hyperplastic change of Kupffer cells eventually containing LPS was found in animals infected with both strains (Fig. 3A and B). The presence of bacteria in the liver after i.v. administration and the consequent microgranuloma formation suggested that shigellae can survive in blood and reach the liver in which they reside and stimulate complex cellular responses.

The spleen of mice that received M90T was activated, displaying large and diffused follicles consisting of white pulp and many PMN cells (data not shown). In contrast, no morphologic alterations were observed in the spleen of mice infected with BS176. Scores about liver damages and spleen activation are shown in Table 1.

Mice mortality relies on Shigella*'s invasiveness*

The findings obtained with M90T and BS176 in both models about organ colonization, persistence and histological features of infected tissues suggested that invasiveness might play a main role in provoking the lesions of the liver that definitely led the infected animals to death. To assess this hypothesis, we analysed the *S. flexneri* mutant M90T Δ*ipaB* (Menard *et al*., 1993) in the i.v. infection model. M90T Δ*ipaB* is a non-invasive M90T mutant as it does not produce IpaB, involved in bacterial internalization in epithelial cells (Menard *et al*., 1993), lysis of the phagocytic vacuole and the activation of caspase-1 in macrophages (Chen *et al*., 1996).

Therefore, 20 mice received 10^7 cfu of M90T Δ*ipaB* and no mortality was observed over 96 h p.i. At 48 h p.i., 10 animals were sacrificed, and the liver and spleen were examined. The numbers of cfu recovered were: 10 for the spleen and 10^3 for the liver. Consistent with the low number of bacteria, histological analysis of these tissues revealed no necrosis (score 0), perihepatitis or neutrophil activation (Fig. 2E and F), and the presence of LPS only in the cytoplasm of the infected cells (Fig. 3C), as well as mild (score 1) splenic activation (Table 1).

M90T induces apoptosis of macrophages within microgranulomas

As apoptosis has been described as a feature of hepatic granulomas after bacterial infection (Matsunaga and Ito, 2000), we analysed for the presence of apoptotic cells within microgranulomatous lesions the livers of mice infected with M90T, BS176 or M90T Δ*ipaB* using the TUNEL experimental approach. Apoptotic cells were observed only in tissues of animals that received M90T

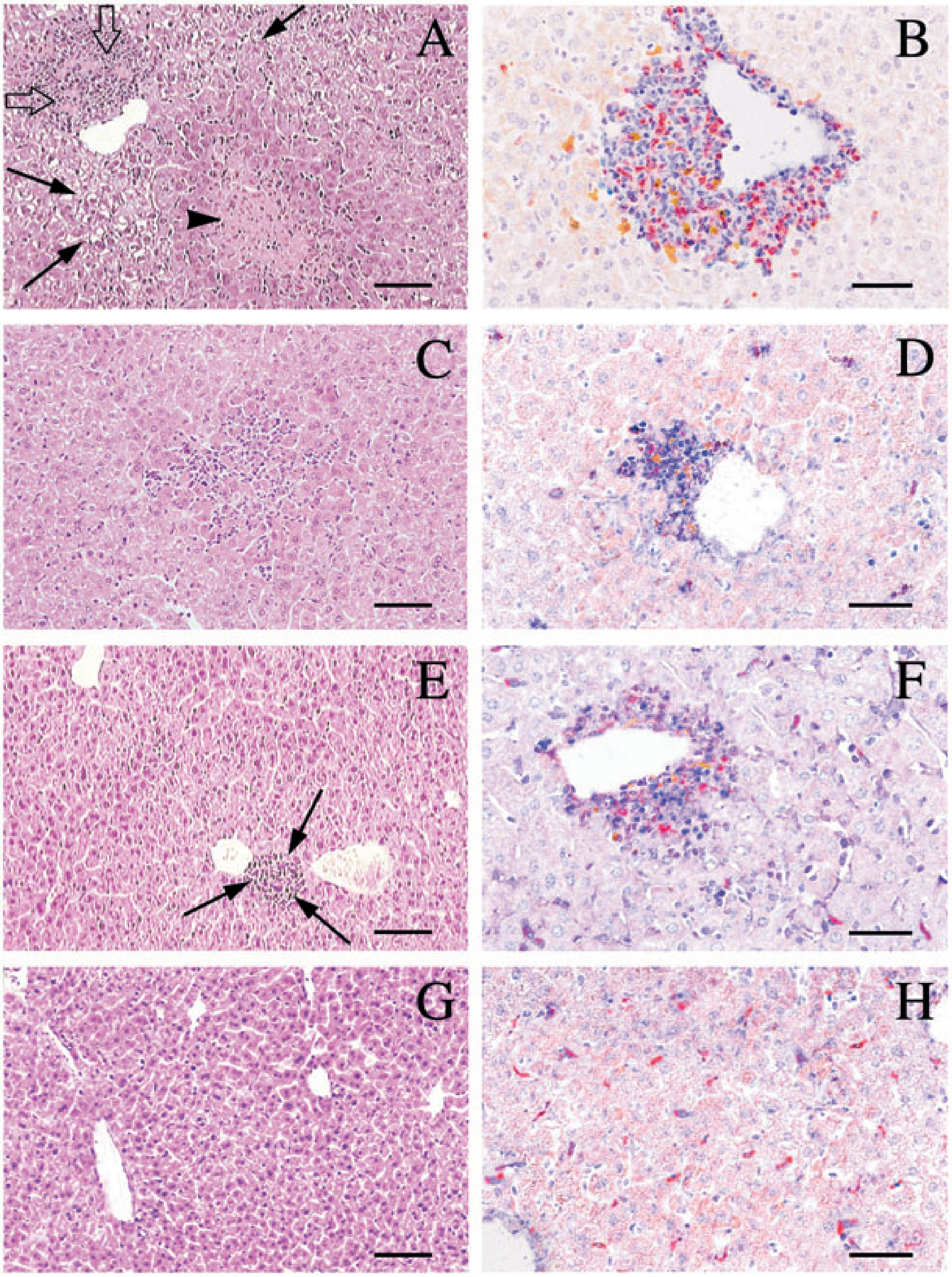

Fig. 2. Histopathological and immunohistochemical analysis of tissue sections of the liver of animals infected with M90T, BS176 and M90T Δ*ipaB* at 48 h post infection (p.i.), and of the liver of an uninfected control mouse. Haematoxylin-eosin staining of sections of murine liver infected with M90T (A), BS176 (C), M90T Δ*ipaB* (E) and a control section (G). Immunohistochemical characterization of principal immunophenotypes (CD3+ lymphocytes and F4/80+ cells) of mononuclear cells involved in mononuclear cell aggregates induced by M90T (B), BS176 (D), M90T Δ*ipaB* (F), eventually containing *S. flexneri* 5 LPS, compared with an uninfected control (H).

A. Severe degeneration and cloudy swelling of hepatocytes (arrows) is accompanied by necrotic areas in which cellular morphology is completely altered (arrowhead). A microgranuloma, resulting in mononuclear cell aggregates with few, interspersed neutrophils, infiltrating into pericentrolobular tract, is present (open arrows).

C and E. The normal structure of hepatic parenchyma is observable. Only small aggregates of macrophages and lymphoid cells are present (arrows in E).

G. Physiological aspect of the liver belonging to an uninfected control mouse. There are no cellular infiltrates between *muralia* of hepatocytes.

B, D, F and H. Many CD3+ lymphocytes (in blue) and macrophages, in some cases positive both for anti-*S. flexneri* LPS mAb (in brown) and for anti-F4/80 mAb (in red), are present, especially in microgranulomas induced by M90T (B). In (H), note the only presence of purple red-stained Kupffer cells in the absence of mononuclear infiltrates. Avidin-biotin immunoperoxidase triple stain method, Mayer's haematoxylin nuclear counterstain.

Scale bars 50 μm (A, C, E and G) and 25 μm (B, D, F and H).

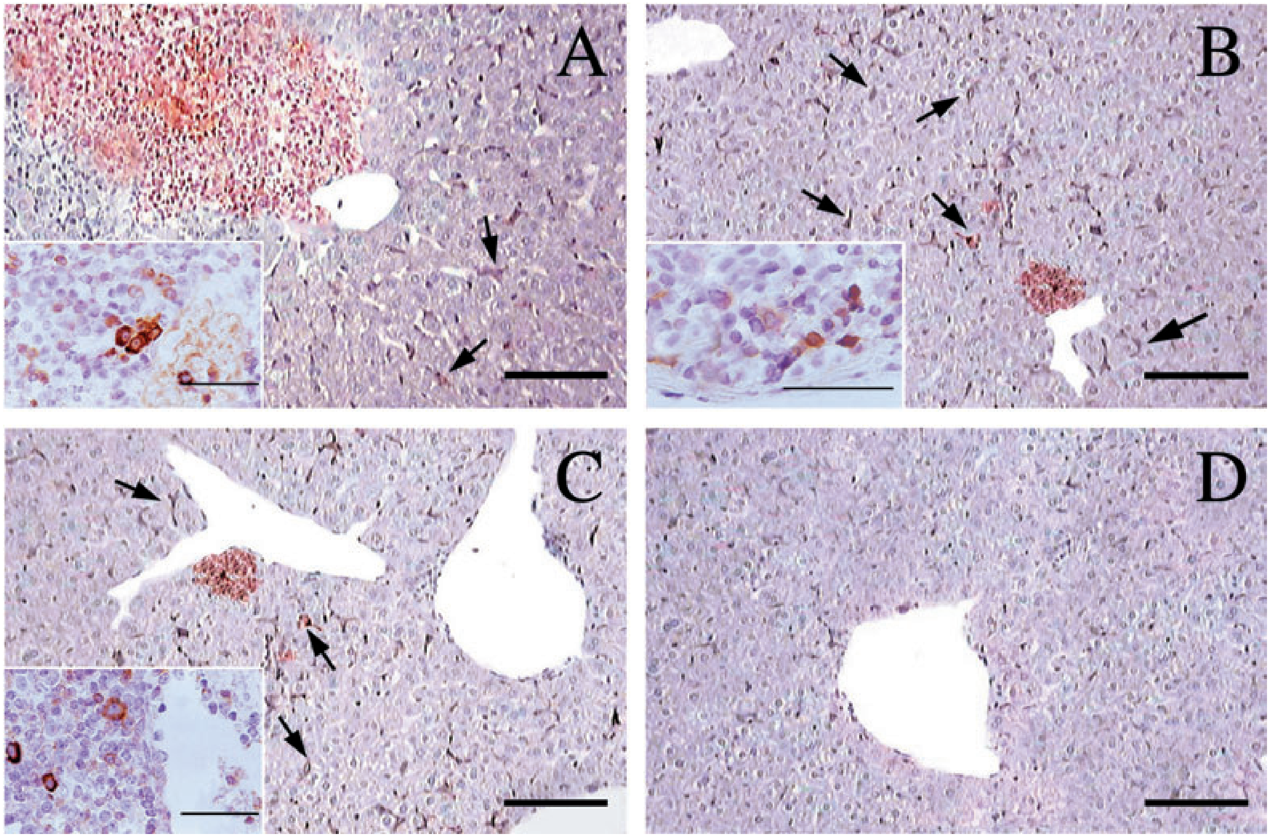

Fig. 3. Immunohistochemical detection of *S. flexneri* 5 LPS in the liver of infected and control mice.
A–C. Immunostaining of serotype 5 somatic antigen by anti-LPS monoclonal immunoglobulin A into microgranulomatous lesions of the liver of mice infected with M90T (A), BS176 (B) and M90T Δ*ipaB* (C).
D. An immunostained section of the liver of an uninfected control mouse is shown.
Note the characteristic localization of the antigen into the cytoplasm of mononuclear cells belonging to macrophage lineage (see inserts of A–C) and into Kupffer cells of the same sections (arrows). Scale bars 25 μm. In inserts, scale bars 15.8 μm.

(Fig. 4A) whereas a small number of apoptotic cells were found in the liver of mice infected with M90T Δ*ipaB* (Fig. 4C). No or a very few apoptotic cells were detected in microgranulomas induced by BS176 (Fig. 4B). In mice infected with M90T, typical apoptotic cells were more frequently observed in microgranulomas rather than in the sinusoidal inflammatory cells, i.e. Kupffer cells or hepatocytes. Apoptotic cell death was measured by enumerating

Table 1. Scores related to histological examination of the liver and the spleen of mice infected with *S. flexneri* M90T, BS176 or M90T Δ*ipaB*.

	Parameter in the liver								
Strain	Necrosis[a]	Microgranulomas[b]	Perihepatitis[c]	Neutrophils[d]	Mononucleates[d]	Degeneration[e]	Intracytoplasmic LPS[f]	Free LPS[g]	Spleen activation[h]
M90T	2	3	0	2	2	3	3	3	3
BS176	0	1	0	0	1	0	2	0	0
M90TΔ*ipaB*	0	1	0	0	1	1	2	0	1
Control	0	0	0	0	0	0	0	0	0

a. Extension of necrotic areas.
b. Number of hepatic microgranulomas: 1 = few, 2 = several, 3 = many.
c. Degree of involvement of Glissonian capsule.
d. Score as cells per high-power field (HPF) at ×400 magnification: 1 = 5–19 cells, 2 = 20–49 cells, 3 = 50 cells or more.
e. Degree of hepatocytic degeneration, i.e. cloudy swelling, vacuolar degeneration.
f. Degree of intracytoplasmic LPS positivity in microgranulomas' central mononucleates.
g. Degree of LPS positivity throughout the hepatic parenchyma.
h. Degree of white pulp activation (aspecific), mainly due to PMN cells.

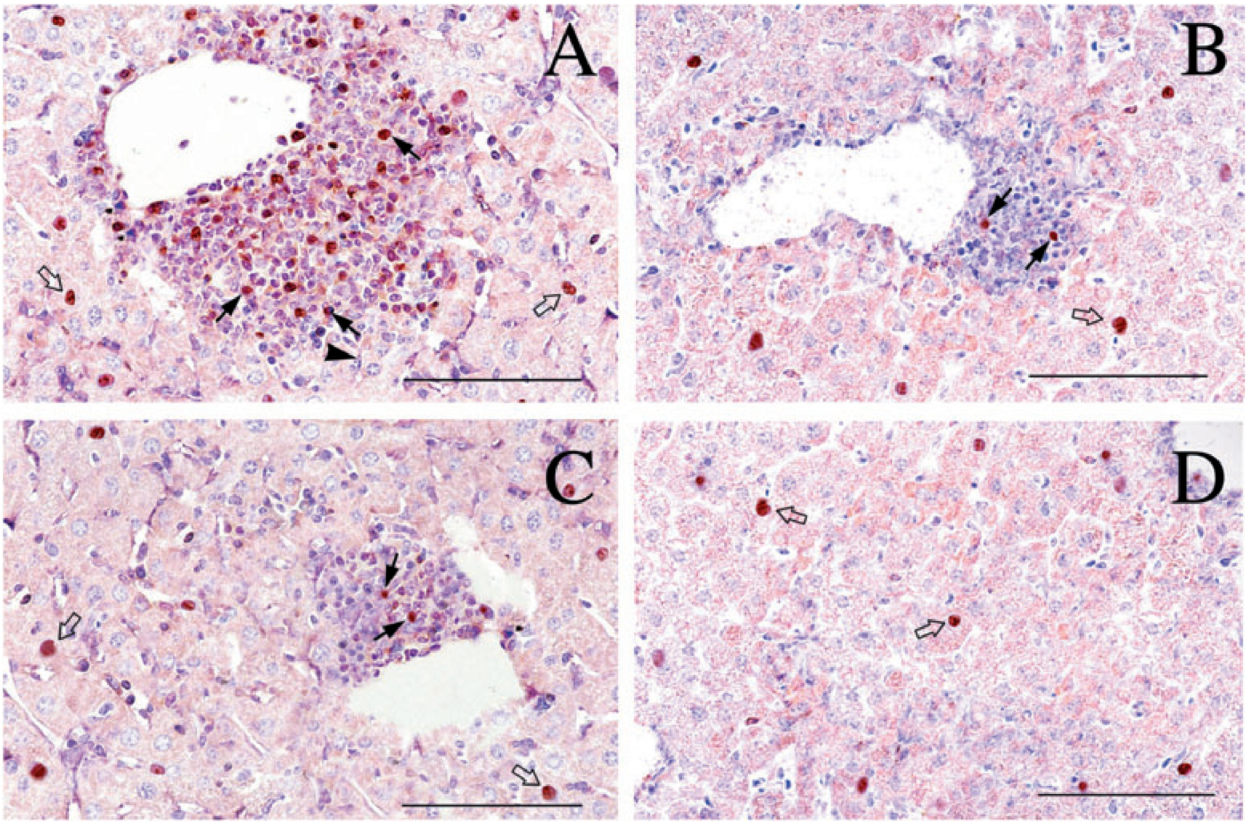

Strains	Mean apoptotic index
M90T	66.8 ± 9.30
BS176	1.22 ± 0.99
M90T Δ*ipaB*	4.32 ± 2.74
Control	0.003

Fig. 4. Apoptosis assessment.
Top. TUNEL analysis showing the presence of apoptotic cells within microgranulomatous lesions of the liver of mice infected with M90T, BS176 or M90T Δ*ipaB*, and in the corresponding areas of an uninfected control. A. High number of TUNEL-positive nuclei are observed in mononuclear cells (arrows), hepatocytes (open arrows) and Kupffer cells (arrowhead) of mice that received M90T. B and C. Only sporadic apoptotic cells are present in mononuclear cell infiltrates of the liver of mice infected with BS176 and M90T Δ*ipaB* respectively (arrows). Note the low number of apoptotic hepatocytes in perigranulomatous areas of these liver sections (open arrows). D. A physiological number of hepatocytes that showed apoptotic activity in a liver section of an uninfected control mouse are evident. Scale bars 25 μm.
Bottom. Apoptotic index in the liver of mice infected with M90T, BS176 and M90T Δ*ipaB*. The mean apoptotic index is defined as the percentage of TUNEL-positive nuclei over the total number of cells within microgranulomas in liver tissue samples of mice infected with the different strains. A minimal of 10 fields per samples were analysed at ×40. BS176 versus M90T: $P < 0.0001$ by Student's *t*-test. M90T DipaB versus M90T: $P < 0.0001$ by Student's *t*-test. The control value represents the mean percentage of TUNEL-positive cells calculated as above over a same number of cells in the corresponding areas of the uninfected animals.

the TUNEL-positive cells in the liver of infected mice (Fig. 4, bottom).

M90T provokes acute liver failure and hepatic injury

To evaluate the correlation of apoptotic index with the degree of hepatocellular swelling and acute liver failure, we measured aspartate aminotransferase (AST), alanine aminotransferase (ALT) and total protein levels in sera of mice infected with different strains. At 24 h after *S. flexneri* challenge, all the infected animals exhibited an increase in AST and ALT serum levels (Table 2). At 48 h p.i., the level of AST and ALT in animals receiving BS176 and M90T Δ*ipaB* reached the same level as in

Table 2. Hepatic transaminases and total protein levels of mice infected with *S. flexneri* M90T, BS176 or M90T Δ*ipaB* at 24 and 48 h p.i.

Strain	M90T		BS176		M90T Δ*ipaB*		Control	
Time post infection (h)	24	48	24	48	24	48	24	48
AST (U l^{-1})	199 ± 31.2	2697 ± 343	78.1 ± 20.3	88.6 ± 18.4	73.7 ± 39.9	68.4 ± 21.3	44.2 ± 15,3	50.8 ± 11.4
ALT (U l^{-1})	124 ± 29.4	508 ± 76.9	22.3 ± 3.9	20.4 ± 2.1	24.3 ± 13.2	26.7 ± 12.1	19.3 ± 12.1	18.0 ± 2.9
Total proteins (g dl^{-1})	4.15 ± 0.43	4.62 ± 0.95	5.57 ± 0.87	6.13 ± 1.02	5.77 ± 0.75	5.10 ± 0.65	5.40 ± 0.97	4.14 ± 0.99

Data are pooled results of three experiments. Values are geometric mean ± SEM ($n = 6$ for each strain, including controls, and time point in each experiment).
AST, aspartate aminotransferase; ALT, alanine aminotransferase.

uninfected controls. In contrast, in mice infected with M90T, the level of transaminases increased dramatically between 24 and 48 h, and reached values ≈53 times greater than those of the controls thus indicating drastic failure of hepatic parenchyma. These results are consistent with the peak of apoptotic cells in microgranulomas at the same time point (48 h p.i.) and, at the histological level, with the cytolytic or coagulative necrosis of hepatocytes observed.

Expression of multiple cytokines in the liver of infected animals and production of cytokine IL-6

To gain insight into the inflammatory process induced by *S. flexneri* in the liver, the expression of relevant cytokines was investigated by reverse transcription polymerase chain reaction (RT-PCR). We analysed the expression of TNF-α, IL-1β, IL-6, IL-18 and IFN-γ at 24 and 48 h p.i. (Fig. 5). In uninfected livers, no cytokine expression was recorded with the exception of IL-12. IL-1β mRNA was mainly produced at 24 and 48 h after M90T infection. No or a very small amount of mRNA for this cytokine was detected with BS176 and M90T Δ*ipaB.* At 48 h p.i., a certain degree of decrease in IL-12 mRNA production was observed in the liver of animals infected with all strains. The three strains induced a significant expression of IL-18, especially M90T at 24 h p.i. A low level of IFN-γ mRNA was found at 24 h p.i. with M90T and BS176 whereas M90T Δ*ipaB* induced a high level of this mRNA. The strains induced a variable expression of TNF-α. At 24 h p.i., a significant amount of this mRNA was revealed with M90T, whereas null and minimal level was observed after BS176 and M90T Δ*ipaB* challenge respectively. At 24 and 48 h p.i., a good production of TNF-α mRNA was detected in livers infected by M90T whereas no production was found in the liver of animals infected with the other strains. IL-6 is considered to be a relevant marker of inflammation in mice. The mRNA for this cytokine was only produced at 24 h p.i. in the liver of animals infected with M90T. Similarly, this cytokine in blood was only evident at 24 h p.i. in mice infected with this strain (Fig. 6).

Discussion

The premise of this study is the assumption that it is not necessary for a model of infection to mimic every aspect of a natural disease. Moreover, it is necessary to determine which features are mimicked accurately. Two new concepts emerge from this model of *Shigella* infection: (i) i.v. administration of a relatively small amount of virulent shigellae induces death in mice and (ii) there is evidence that the liver may be an important target for *Shigella* infection. The association of *S. flexneri* enteritis with hepatitis – documented by the elevated transaminase and alkaline phosphatase levels – whose persistence coincides with the presence of and whose cut-down coincides with the cessation of acute diarrhoea has been described (Stern and Gitnik, 1976). Likewise, after *Shigella dysenteriae* infection in humans (Levine *et al.*, 1974) and in rodent models (Nofech-Mozes *et al.*, 2000), sepsis and abnormal liver function tests, as well as high levels of mRNA for TNF-α and IL-1β in the liver, were reported respectively.

We found that less than 1 h after i.v. injection, invasive and non-invasive shigellae reach the liver where they survive and proliferate depending on their virulence. The immediate effect of their presence is microgranuloma formation. Primary granulomatous response serves to prevent pathogen spread, as in *Mycobacterium* and some fungi (Matsunaga and Ito, 2000) infections. During early stages of granuloma formation, monocyte-derived macrophages infiltrate the hepatic sinusoids where Kupffer cells, acting as the first-line host defence, prevent the spread of infectious agents (Yamaoka *et al.*, 1996). These cells can autonomously replicate and differentiate into activated macrophages that participate in granuloma formation (Naito and Takahashi, 1991; Takahashi *et al.*, 1994). In our model, live bacteria transported by bloodstream undergo phagocytosis by Kupffer cells and perisinusoidal macrophages. We found that these cells form a component of well-organized microgranulomas in pericentrolobular space. Therefore, microgranulomas might play a physiological role in limiting *Shigella* colonization of the liver. However, this does not seem to be the case with the

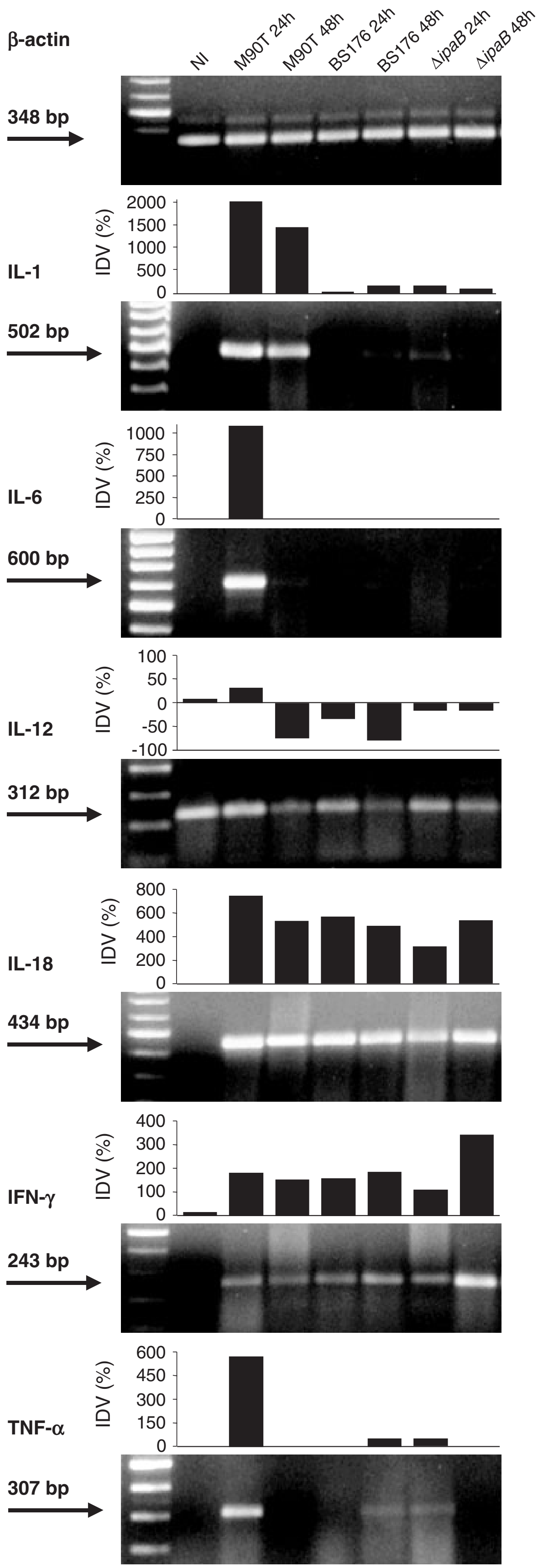

Fig. 5. RT-PCR and densitometry products of RNAs extracted from the liver of mice infected with M90T, BS176 or M90T Δ*ipaB*, using primers specific for β-actin, IL-1β, IL-6, IL-12, IL-18, IFN-γ and TNF-α at 24 and 48 h p.i. The intensity of the bands was quantified and normalized for β-actin and expressed as per cent of increase or decrease of the value obtained with the non-infected control taken as 0. IDV = Integrated Density Values ($n = 6$ for each experimental time point). Similar results were obtained in three identical experiments. Standard deviations for three experiments were within 10% of IDV.

wild-type strain. In fact, at 48 h p.i. in the presence of microgranulomas the few surviving animals exhibit a severe failure of hepatic function characterized by a dramatic increase of transaminases in blood and, at the histopathological level, extensive hepatocyte necrosis. The non-invasive variant, BS176, and the M90T Δ*ipaB* mutant still provoke the formation of microgranulomas, although of a smaller size than those produced by the wild-type strain. However, BS176 and M90T Δ*ipaB* mutant do not induce death of the infected animals, and transaminase levels only rise transiently in accordance with the reduced damages in hepatic parenchyma. This suggests that microgranulomas by themselves are not sufficient to prevent *Shigella* dissemination in the liver and that other mechanisms might participate to clearance of the pathogens from this organ.

It has been reported that apoptosis of infected macrophages in microgranulomas plays a crucial role in the host defence against intracellular microorganisms such as different species of *Mycobacterium* (Molloy *et al*., 1994; Fratazzi *et al*., 1997). In this case, factors released by activated macrophages, i.e. reactive oxygen intermediates and TNF-α (Moss *et al*., 1999), might trigger the death signalling pathway initiated by TNF-α–TNF-α receptor 1 interaction (Keane *et al*., 1997). In this respect, the presence of a high apoptotic index in macrophages con-

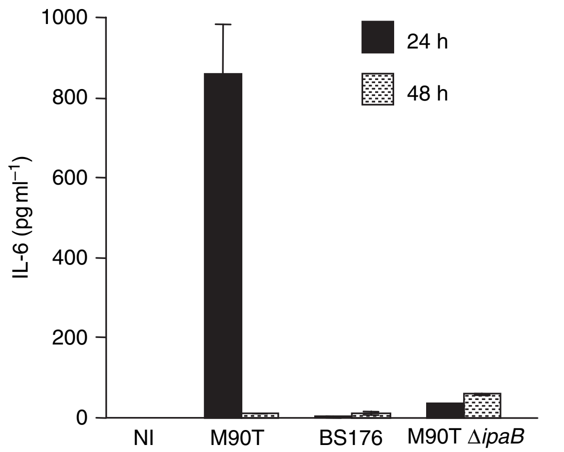

Fig. 6. IL-6 production by mice infected with *Shigella* strains. IL-6 levels were determined in the serum of mice infected with M90T, BS176 or M90T Δ*ipaB* at 24 and 48 h p.i. and expressed in pg ml^{-1}. Values are geometric mean ± SEM ($n = 10$).

stituting granulomas may be considered beneficial for host defence. In our model, granuloma formation, increase in transaminase level, augmented production of mRNA for IL-1β, TNF-α and IL-6 as well as high IL-6 level in blood together with necrotic areas in the hepatic tissue are all features associated with high apoptotic index observed in the liver of M90T-inoculated animals at 48 h p.i. Both the non-invasive variant BS176 and the M90T Δ*ipaB* mutant, which does not produce the invasin IpaB responsible for caspase-1 activation, do not provoke macrophage death (Hilbi *et al*., 1998). This is in agreement with the low apoptotic index displayed by these strains in the hepatic tissue. Therefore, in our case the high apoptotic index observed in the hepatic tissue of animals infected with M90T does not predict a good outcome from infection but it might be a marker of disease severity.

In the model of bacterium-induced fulminant hepatitis (Wyke *et al*., 1982), the characteristic massive hepatic necrosis occurs in two phases: the early priming phase induced by the injection of inactivated bacteria, e.g. *Propionibacterium acnes*, and the late excitation phase elicited by LPS administration (Ferluga and Allison, 1978; Mizoguchi *et al*., 1988; Nagakawa *et al*., 1990). During the priming phase, mononuclear cells infiltrate the liver lobules over a few days, leading to granuloma formation in which activated macrophages are present. Subsequent LPS injection causes acute lethality with massive hepatocellular damage characterized by hepatocellular loss due to apoptosis and necrosis. We hypothesize that our model of i.v. infection in mice includes both these phases, culminating in a fulminant hepatitis. In the first phase, *Shigella* captured by Kupffer cells induce the granuloma organization; both invasive and non-invasive strains provoke an increase of transaminases. In the liver of animals infected with M90T, we may observe a second phase characterized by macrophage apoptosis that initiates the secondary phase during which damaged macrophages release *Shigella* LPS or live bacteria. According to the fulminant hepatitis model, apoptosis can induce the production of pro-inflammatory mediators such as IL-1β, but also IL-6 and TNF-α, which play a crucial role in provoking massive destruction of hepatocytes (seen by severe increase of ALT and AST levels and dramatic lethality). Moreover, this *in situ* release of LPS and living shigellae might further promote apoptosis, thus amplifying the process. In contrast, the 'eliciting' phase is absent or hardly present when animals are infected with mutants unable to provoke apoptosis. In this instance, the microgranulomas might play their physiological role in successfully blocking the dissemination of the bacteria (Fig. 7).

In conclusion, the emerging concept that pathogenesis of natural shigellosis relies on the inflammation mainly elicited by macrophage, monocyte and dendritic cell apoptosis (Zychlinsky *et al*., 1992; Edgeworth *et al*., 2002; Hathaway *et al*., 2002) and the subsequent release of IL-1β and IL-18 is supported by this new model of infection.

The i.v. model is reproducible, and the results obtained with a range of mutants altered in different steps of pathogenesis are consistent with other infection models (M.L. Bernardini *et al*., unpubl. results). The findings here reported and particularly the relevant expression of mRNA for cytokines in the liver encourage to further dissect the liver's response after i.v. injection of shigellae in order to exploit this animal model to study the T-cell-mediated response to *Shigella* infection. In fact, in the granulomatous lesions the cellular complexes, constituted by macrophages and epithelioid cells, recruit T-cells followed by myeloid effector cells. These lesions represent a productive model to study T-cell-mediated immunity (Co *et al*., 2004) and they have been extensively exploited to study several processes associated with T-lymphocytes such as the characterization of IL-4 producing CD8+ T-cells (Salgame *et al*., 1991) and the identification of γδ-T-lymphocytes (Modlin *et al*., 1989). Moreover, this model benefits of a clear read-out which may be advantageous in evaluating a range of reagents useful to inhibit the different phases of the inflammatory response. Finally, the availability of knock-out mice and of mice expressing human genes might make the i.v. injection of shigellae a reliable model to study pathologies of the liver beyond the specific context of shigellosis.

Experimental procedures

Bacterial strains, growth conditions and genetic procedures

The *S. flexneri* 5a strains used in this study are the wild-type M90T [streptomycin (Sm) resistant] (Allaoui *et al*., 1992), its non-invasive variant BS176 (lacking the virulence plasmid pWR100) (Sansonetti *et al*., 1982; Buchrieser *et al*., 2000) and M90T Sm^R Δ*ipaB* [kanamycin (Km) resistant] (Menard *et al*., 1993). All strains were routinely grown on trypticase soy broth (TSB) (Becton Dickinson and Co.), trypticase soy agar (1.2% agar) (TSA) (Difco Laboratories) or Luria–Bertani broth (LB) (Miller, 1992). TSA containing 100 mg of Congo red dye (Cr) per litre was used to select Cr^+ clones of *Shigella* spp. (Maurelli *et al*., 1984). Hektoen enteric agar (HEA) (Oxoid) was used to grow shigellae recovered from the infected organs. When necessary, Sm (100 μg ml^{-1}) or Km (30 μg ml^{-1}) (all from Sigma Chemical) were added to bacterial cultures.

Mice

Outbred 5-week-old female BALB/C mice (Charles River Italia) were used for i.v. inoculation. All animals were housed 10 per cage at the Regina Elena Institute animal care facility.

Intravenous inoculation

Mice received food and water *ad libitum*. Isolated Cr^+ (red) *Shigella* colonies grown on Cr-TSA plates were inoculated in 1 ml

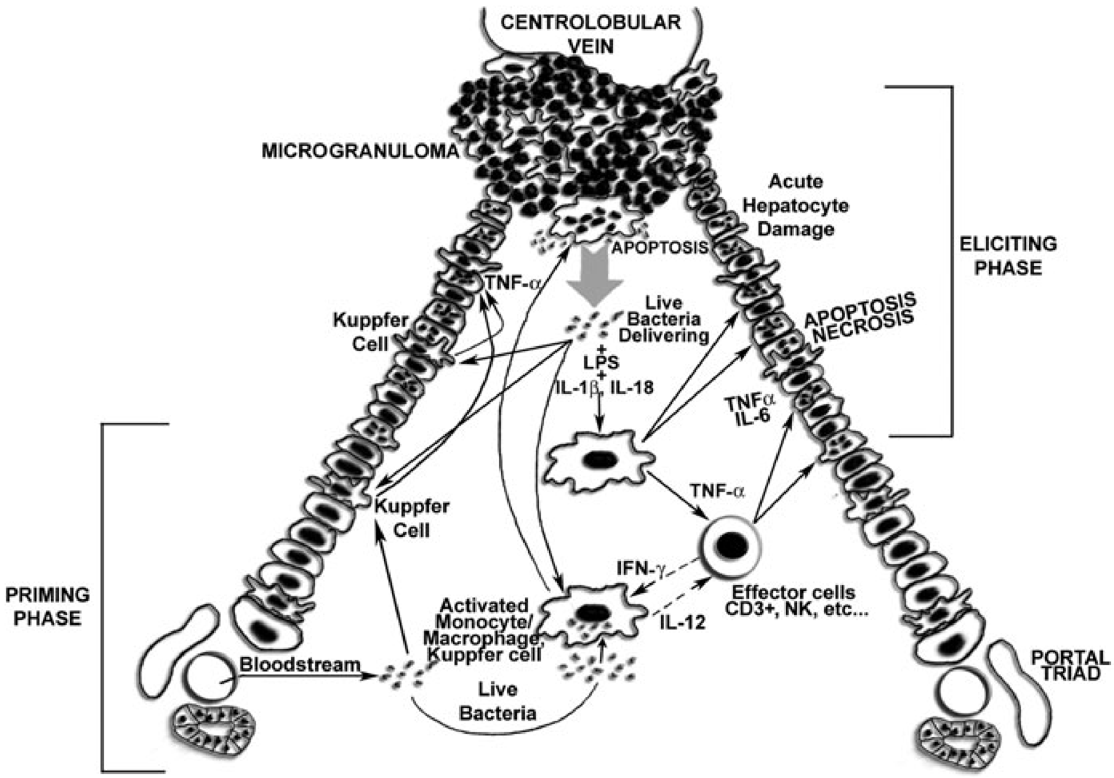

Fig. 7. Scheme of a possible process leading to hepatic injury after i.v. infection with *S. flexneri* wild-type strain. This design is a schematic view of a functional hepatic lobule in which the centrolobular vein and two hepatic triads are evidenced. In the priming phase, wild-type *Shigella* transported through sinusoids in the liver induce mononuclear cell infiltrate leading to microgranuloma formation. Upon contact with shigellae, macrophages present in the microgranulomas undergo caspase-1-mediated apoptosis, which is accompanied by the release of high levels of IL-1β, bacterial LPS and eventually living shigellae. This process elicits the late excitation phase in which massive damage of previously sensitized hepatocytes occurs.

of LB, with which a TSA-Sm plate was flooded and incubated overnight at 37°C. After 16 h of growth, 1 ml of sterile saline solution (SSS) was used to resuspend the bacterial layer, and appropriate dilutions were made to achieve the desired inoculum. Mice were challenged by injection of the caudal vein with 200 μl of bacterial suspension in each experiment (BD Microlance 3, 0.4×19, Nr.20) and deaths were recorded for 4 consecutive days. Each experiment was repeated at least three times. Uninfected mice having received 200 μl of SSS through the caudal vein were used as controls in each experiment.

Survival studies

Cages were inspected twice daily. At the desired time points, animals were sacrificed by cervical dislocation.

Recovery of shigellae from tissues of infected mice

The abdominal cavity was aseptically opened and the spleen and the liver were removed and prepared for histopathology, RT-PCR studies and counts of viable bacteria. For bacterial counts, tissues were placed in sterile tubes containing cold SSS (5 ml for liver and 2 ml for spleen) and stored on ice until further manipulation. Tissues were then homogenized (Ultra Turrax IKA T18 Basic) and serial dilutions were plated on HEA. Bacterial counts were normalized to the dilution factor and reported as cfu per organ.

Histopathology

Samples for histological and immunohistochemical analyses were fixed in 10% buffered formalin and paraffin embedded. Three-micrometre-thick sections were stained with haematoxylin-eosin (HE) for histopathological examination. To localize *S. flexneri* antigen in infected tissues and to characterize the cell populations involved in inflammation, the following mAbs were used on serial sections: immunoglobulin A (IgA) mAb anti-*S. flexneri* 5a LPS (6 mg ml^{-1}; A. Phalipon, Institut Pasteur, Paris, France), rat mAb anti-murine CD3+ lymphocytes (Serotec), rat mAb anti-murine macrophages (F4/80 antigen, Serotec). Pro-apoptotic effect provoked by *S. flexneri* in microgranulomas was highlighted with a TUNEL colorimetric staining (Apoptag, Intergen or DeadEnd, Promega) in which DNA fragments were visualized by digoxigenin nucleotide labelling and revealed by an anti-digoxigenin antibody conjugated with peroxidase, according to the manufacturer's instructions.

For immunohistochemical tests, sections were placed onto pretreated slides (Bio-Optica) and dried overnight at 37°C. After being dewaxed, sections were placed in EDTA buffer, pH 9.0, and processed in a microwave oven at 650 W for two cycles of 10 min each and cooled at room temperature for 20 min. Tissue sections were then incubated overnight in a moist chamber at 4°C with different primary antibodies, diluted 1:50 in Tris-buffered solution (TBS) containing 0.1% crystalline bovine serum albumin (BSA). Binding of mAb was revealed with ABC-peroxydase or ABC-alkaline phosphatase techniques using 1:200 diluted biotinylated conjugated rabbit anti-rat immunoglobulin G (IgG; all from Vector Laboratories) and a 1:200 diluted biotinylated goat anti-mouse Ig (AO433; DAKO), applied for 45 min at room temperature, as secondary antibodies. The enzymatic reaction was developed with 3-1-diaminobenzydine (DAB) (Sigma), VIP or Vector Blue, and Vector Red (all from Vector) as substrates, respectively, for ABC-peroxydase and ABC-alkaline phosphatase techniques. For triple staining, the chromogens used were, respectively, DAB, VIP and Vector Blue, with Meyer haematoxylin used as nuclear counterstain. Specific primary antibodies substituted with TBS or non-immune sera were used as negative controls. Histological examination included assessment of inflammation by scoring the number of inflammatory cells (macrophages and neutrophils) assessed at ×400 magnification and reported as the mean for the entire specimen. Neutrophils were classified as absent (score 0) with none or only single sporadic cells per high-power field (HPF), mild (score 1) for a few cells (5–19) per HPF, moderate (score 2) for several cells (20–49) per HPF or severe (score 3) for 50 cells or more per HPF. The quantity of mononuclear cells was considered normal when none or only a few cells were seen in an HPF (score 0). Increase in the number of cells was considered mild for specimens with several cells per HPF (score = 1), moderate (score = 2) for many cells per HPF or severe (score = 3) for numerous cells per HPF. Moreover, tissue changes (i.e. cloudy swelling of hepatocytes and areas of degeneration or necrosis) as well as perivascular and/or parenchymal spots of inflammatory cell aggregates were recorded and expressed with similar scores.

Microgranuloma was defined as a well-circumscribed cell aggregation composed of five or more mononuclear phagocytes. The number of TUNEL-positive cells was assessed under a dry-X40 objective. The total number of cells constituting the microgranulomas or the small mononuclear infiltrate was recorded as well as the number of TUNEL-positive cells. Results were reported as the mean of the percentages of positive cells with respect to the total number of cells of microgranulomatous lesions for the entire specimen. The number of TUNEL-positive cells calculated over a same number of cells in the corresponding areas of the uninfected animals was used as a control.

Determination of serum GPT (ALT), GOT (AST) and total protein levels

Serum glutamic piruvic transferase (GPT) (ALT), glutamic oxal-acetic transferase (GOT) (AST) and total proteins count levels were determined in sera of animals infected with *Shigella* strains at 24 and 48 h p.i. with a Fuji DRI-CHEM 5500 V as instructed by the manufacturer (Fuji Medical System).

Tissue cytokines' measurements

Livers were removed at 24 and 48 h p.i., dissected aseptically, immersed immediately in liquid nitrogen and stored at –80°C. Total RNA from homogenized tissues was extracted using Trizol solution (Invitrogen Italia), in accordance with the manufacturer's instructions. RNAse-free DNAse (Boehringer Mannheim) was used to remove genomic DNA (Dilworth and McCarrey, 1992). Reverse transcription of total RNA (1 μg) and cDNA PCR was performed by using the Super-Script™ One-Step RT-PCR with Platinum Taq (Invitrogen Italia) in accordance with the manufacturer's instructions. Gene-specific primers are: forward, 5′-TGGAATCCTGTGGCATCCATGAAAC-3′ and reverse, 5′-TAAAACGCAGCTCAGTAACAGTCCG-3′ for β-actin; forward, 5′-TCATGGGATGATGATGATAACCTGCT-3′ and reverse, 5′-CCCATACTTTAGGAAGACACGGATT-3′ for IL-1β; forward, 5′-CTGGTGACAACCACGGCCTTCCCTA-3′ and reverse, 5′-ATGCTTAGGCATAACGCACTAGGTT-3′ for IL-6; forward, 5′-AGCGGCTGACTGAACTCAGATTGTAG-3′ and reverse, 5′-GGCAGGTCTACTTTGGAGTCATTGC-3′ for IFN-γ; forward, 5′-GGCAGGTCTACTTTGGAGTCATTGC-3′ and reverse, 5′-ACATTCGAGGCTCCAGTGAATTCGG-3′ for TNF-α; forward, 5′-ACCGAATTCACTGTACAACCGCAGTAATACGGA-3′ and reverse, 5′-GCCTCTAGAGTGAACATTACAGATTTATC CCCA-3′ for IL-18.

PCR mixtures contained 0.2 μM of each primer, two units Platinum Taq, 1.2 mM $MgSO_4$ and 1.2 mM dNTPs. cDNA synthesis was performed at 48°C for 45 min, followed by 94°C for 2 min. PCR using primers for β-actin was performed on each individual sample as an internal positive control standard. As a negative control, PCR in which water substituted cDNA was run concurrently. Cytokine mRNAs were quantified by using a Quantity-one software (Bio-Rad) and results were normalized to the amount of β-actin mRNA. The median value of three runs was used to estimate mRNA levels for individual mice.

ELISA measurements

Peripheral blood from infected BALB/C mice was obtained from the caudal vein, and serum was collected 24 and 48 h p.i. IL-6 levels were determined by solid-phase enzyme-linked immunosorbent assay (ELISA) (R and D Systems). The absorbance was measured at 450 nm, and concentrations were determined by interpolation of a standard calibration curve.

Acknowledgements

We thank the colleagues of the EU-Innovax Network for helpful discussion, Armelle Phalipon for mAbs, Claude Parsot for the gift of M90T Δ*ipaB*, Giorgina Levi for help in the preparation of the manuscript, Christopher Tang for critical reading of the manuscript and Giuseppe Bertini and Piero Piccoli for animal care. This work was supported by grants from the European Commission (QLK2-1999-00938) and the Italian Ministero dell'Istruzione, Università e Ricerca (PRIN 2002).

References

Allaoui, A., Mounier, J., Prevost, C., Sansonetti, P.J., and Parsot, C. (1992) *ics*B: a *Shigella flexneri* virulence gene necessary for the lysis of protrusions during intercellular spread. *Mol Microbiol* **6:** 1605–1616.

Bernardini, M.L., Arondel, J., Martini, I., Aidara, A., and Sansonetti, P.J. (2001) Parameters underlying successful protection with live attenuated mutants in experimental shigellosis. *Infect Immun* **69:** 1072–1083.

Buchrieser, C., Glaser, P., Rusniok, C., Nedjari, H., D'Hauteville, H., Kunst, F., *et al.* (2000) The virulence plasmid pWR100 and the repertoire of proteins secreted by the type III secretion apparatus of *Shigella flexneri*. *Mol Microbiol* **38:** 760–771.

Buttner, D., and Bonas, U. (2002) Port of entry: the type III secretion translocon. *Trends Microbiol* **10:** 186–192.

Chen, Y., Smith, M.R., Thirumalai, K., and Zychlinsky, A. (1996) A bacterial invasin induces macrophage apoptosis by binding directly to ICE. *EMBO J* **15:** 3853–3860.

Co, D.O., Hogan, L.H., Il-Kim, S., and Sandor, M. (2004) T cell contributions to the different phases of granuloma formation. *Immunol Lett* **92:** 135–142.

Dilworth, D.D., and McCarrey, J.R. (1992) Single step elimination of contaminating DNA prior to reverse transcriptase PCR. *PCR Meth Appl* **1:** 279–282.

Edgeworth, J.D., Spencer, J., Phalipon, A., Griffin, G.E., and Sansonetti, P.J. (2002) Cytotoxicity and interleukin-1beta processing following *Shigella flexneri* infection of human monocyte-derived dendritic cells. *Eur J Immunol* **32:** 1464–1471.

Etheridge, M.E., Hoque, A.T., and Sack, D.A. (1996) Pathologic study of a rabbit model for shigellosis. *Lab Anim Sci* **46:** 61–66.

Ferluga, J., and Allison, A.C. (1978) Role of mononuclear infiltrating cells in pathogenesis of hepatitis. *Lancet* **ii:** 610–611.

Fernandez, M.I., Thuizat, A., Pedron, T., Neutra, M., Phalipon, A., and Sansonetti, P.J. (2003) A newborn mouse model for the study of intestinal pathogenesis of shigellosis. *Cell Microbiol* **5:** 481–491.

Formal, S.B., Kundel, D., Schneider, H., Kunev, N., and Sprinz, H. (1961) Studies with *Vibrio cholerae* in the ligated loop of the rabbit intestine. *J Exp Pathol* **42:** 504–510.

Fratazzi, C., Arbeit, R.D., Carini, C., and Remold, H.G. (1997) Programmed cell death of *Mycobacterium avium* serovar 4-infected human macrophages prevents the mycobacteria from spreading and induces mycobacterial growth inhibition by freshly added, uninfected macrophages. *J Immunol* **158:** 4320–4327.

Girardin, S.E., Boneca, I.G., Carneiro, L.A., Antignac, A., Jehanno, M., Viala, J., *et al.* (2003) Nod1 detects a unique muropeptide from Gram negative bacterial peptidoglycan. *Science* **300:** 1584–1587.

Hathaway, L.J., Griffin, G.E., Sansonetti, P.J., and Edgeworth, J.D. (2002) Human monocytes kill *Shigella flexneri* but then die by apoptosis associated with suppression of proinflammatory cytokine production. *Infect Immun* **70:** 3833–3842.

Hilbi, H., Moss, J.E., Hersh, D., Chen, Y., Arondel, J., Banerjee, S., *et al.* (1998) *Shigella*-induced apoptosis is dependent on caspase-1 which binds to IpaB. *J Biol Chem* **273:** 32895–32900.

Keane, J., Balcewicz-Sablinska, M., Remold, H., Chupp, G.L., Meek, B.B., Fenton, M.J., and Kornfeld, H. (1997) Infection by *Mycobacterium tubercolosis* promotes human alveolar macrophage apoptosis. *Infect Immun* **65:** 298–304.

Kotloff, K.L., Winickoff, J.P., Ivanoff, B., Clemens, J.D., Swerdlow, D.L., Sansonetti, P.J., *et al.* (1999) Global burden of *Shigella* infections: implication for vaccine development and implementation. *WHO Bull* **77:** 651–666.

Levine, V.D., Overtruf, G.D., and Mathies, A.W. (1974) *Shigella dysenteriae* type 1: severe dysentery and sepsis with hematologic, hepatic and renal complications. *Western J Med* **121:** 501–504.

Mandic-Mulec, I., Weiss, J., and Zychlinsky, A. (1997) *Shigella flexneri* is trapped in polymorphonuclear leukocyte vacuoles and efficiently killed. *Infect Immun* **65:** 110–115.

Matsunaga, K., and Ito, M. (2000) Quantitative analysis of apoptotic cell death in granulomatous inflammation induced by intravenous challenge with *Cryptococcus neoformans* and bacillus Calmette-Guérin vaccine. *Pathol Int* **50:** 206–218.

Maurelli, A.T., Blackmon, B., and Curtiss, R., III (1984) Temperature-dependent expression of virulence genes in *Shigella* species. *Infect Immun* **43:** 195–201.

Menard, R., Sansonetti, P.J., and Parsot, C. (1993) Nonpolar mutagenesis of the *ipa* genes defines IpaB, IpaC and IpaD as effectors of *Shigella flexneri* entry into epithelial cells. *J Bacteriol* **175:** 5899–5906.

Miller, J.H. (1992) *A Short Course in Bacterial Genetics.* Cold Spring Harbor, NY: Cold Spring Harbor Laboratory Press.

Mizoguchi, Y., Sakagami, Y., Kuboi, H., Kobayashi, K., and Yano, I. (1988) Effects of the polysaccharide in an experimental massive hepatic cells necrosis model. *Biochem Biophys Res Commun* **155:** 1305–1310.

Modlin, R.L., Pirmez, C., Hofman, F.M., Torigian, V., Uyemura, K., Rea, T.H., *et al.* (1989) Lymphocytes bearing antigen-specific gamma delta T-cell receptors accumulate in human infectious disease lesions. *Nature* **339:** 544–548.

Molloy, A., Laochumroonvorapong, P., and Kaplan, G. (1994) Apoptosis, but not necrosis, of infected monocytes is coupled with killing of intracellular bacillus Calmette-Guerin. *J Exp Med* **180:** 1499–1509.

Moss, J.E., Aliprantis, A.O., and Zychlinsky, A. (1999) The regulation of apoptosis by microbial pathogens. *Int Rev Cytol* **187:** 203–259.

Nagakawa, J., Hishinuma, I., Hirota, K., Miyamoto, K., Yamanaka, T., Tsukidate, K., *et al.* (1990) Involvement of tumor necrosis factor-alfa in the pathogenesis of activated-macrophage-mediated hepatitis in mice. *Gastroenterology* **99:** 758–765.

Naito, M., and Takahashi, K. (1991) The role of Kupffer cells in glucan induced granuloma formation in the liver of mice depleted of blood monocytes by administration of strontium-89. *Lab Invest* **64:** 664–674.

Nofech-Mozes, Y., Yuhas, Y., Kaminsky, E., Weizman, A., and Ashkenazi, S. (2000) Induction of mRNA for tumor necrosis factor-alfa and interleukin-1 beta in mice brain, spleen and liver in an animal model of *Shigella*-related seizures. *Isr Med Assoc J* **2:** 86–90.

Perdomo, O.J., Cavaillon, J.M., Huerre, M., Ohayon, H., Gounon, P., and Sansonetti, P.J. (1994) Acute inflammation causes epithelial invasion and mucosal destruction in experimental shigellosis. *J Exp Med* **180:** 1307–1319.

Phalipon, A., Kaufmann, M., Michetti, P., Cavaillon, J.M., Huerre, M., Sansonetti, P.J., and Kraehembuhl, J.P. (1995) Monoclonal immunoglobulin A antibody directed against serotype-specific epitope of *Shigella flexneri* lipopolysaccharide protects against murine experimental shgellosis. *J Exp Med* **182:** 769–778.

Philpott, D.J., Yamaoka, S., Israel, A., and Sansonetti, P.J. (2000) Invasive *Shigella flexneri* activates NF-kappa B through a lipopolysaccharide-dependent innate intracellular response and leads to IL-8 expression in epithelial cells. *J Immunol* **165:** 903–914.

Salgame, P., Abrams, J.S., Clayberger, C., Goldstein, H., Convit, J., Modlin, R.L., and Bloom, B.R. (1991) Differing lymphokine profiles of functional subsets of human CD4 and CD8 T cell clones. *Science* **254:** 279–282.

Sansonetti, P.J., Kopecko, D.J., and Formal, S.B. (1982) Involvement of a plasmid in the invasive ability of *Shigella flexneri*. *Infect Immun* **35:** 852–860.

Sansonetti, P.J., Arondel, J., Fontaine, A., d'Hauteville, H., and Bernardini, M.L. (1991) *ompB* (osmo-regulation) and *icsA* (cell-to-cell spread) mutants of *Shigella flexneri*: vaccine candidates and probes to study the pathogenesis of shigellosis. *Vaccine* **9:** 416–422.

Sansonetti, P.J., Arondel, J., Huerre, M., Harada, A., and Matsushima, K. (1999) Interleukin-8 controls bacterial transepithelial translocation at the cost of epithelial destruction in experimental shigellosis. *Infect Immun* **67:** 1471–1480.

Sansonetti, P.J., Phalipon, A., Arondel, J., Thirumalai, K., Banerjee, S., Akira, S., *et al.* (2000) Caspase-1 activation of IL-1beta and IL-18 are essential for *Shigella flexneri*-induced inflammation. *Immunity* **12:** 581–590.

Sereny, B. (1957) Experimental *Shigella* conjunctivitis. *Acta Microbiol Hung* **2:** 293–296.

Stern, M.K., and Gitnik, G.L. (1976) *Shigella* hepatitis. *JAMA* **235:** 26–28.

Takahashi, K., Naito, M., Umeda, S., and Shultz, L.D. (1994) The role of macrophage colony-stimulating factor in hepatic glucan-induced granuloma formation in the osteopetrosis mutant mouse defective in the production of macrophages colony-stimulating factor. *Am J Pathol* **144:** 1381–1392.

Takeuchi, A., Jervis, H.R., and Formal, S.B. (1975) Animal model of human disease. Bacillary dysentery, shigellosis, *Shigella* dysentery. Animal model: monkey shigellosis or dysentery. *Am J Pathol* **81:** 251–254.

Voino-Yasenetsky, M.V., and Voino-Yasenetskaya, M.K. (1962) Experimental pneumonia caused by bacteria of *Shigella* group. *Acta Microbiol Acad Sci Hung* **11:** 439–454.

Weinrauch, Y., Drujan, D., Shapiro, S.D., Weiss, J., and Zychlinsky, A. (2002) Neutrophil elastase targets virulence factors of enterobacteria. *Nature* **417:** 91–94.

Wyke, R.J., Canalese, J.C., Gimson, A.E., and Williams, R. (1982) Bacteraemia in patients with fulminant hepatic failure. *Liver* **2:** 45–52.

Yamaoka, H., Sakaguchi, N., Sano, K., and Ito, M. (1996) Intravascular granuloma induced by intravenous inoculation of *Cryptococcus neoformans*. *Mycopathologia* **133:** 149–158.

Zychlinsky, A., Prevost, M.C., and Sansonetti, P.J. (1992) *Shigella flexneri* induces apoptosis in infected macrophages. *Nature* **358:** 167–169.

Zychlinsky, A., Fitting, C., Cavaillon, J.M., and Sansonetti, P.J. (1994) Interleukin 1 is released by murine macrophages during apoptosis induced by *Shigella flexneri*. *J Clin Invest* **94:** 1328–1332.